Available online at www.sciencedirect.com
ScienceDirect
Journal of Sound and Vibration 309 (2008) 40–51
JOURNAL OF SOUND AND VIBRATION
www.elsevier.com/locate/jsvi

Secondary actuation and error sensing for active acoustic structure

Kean Chen[a,*], Guoyue Chen[b], Haoran Pan[a], Shuang Li[a]

[a]*Department of Environmental Engineering, College of Marine, Northwestern Polytechnical University, Xi'an, Shaanxi 710072, PR China*
[b]*Faculty of System Science and Technology, Akita Prefectural University, 84-4 Ebinokuchi, Tsuchiya, Honjo, Akita 015-0055, Japan*

Received 15 September 2005; received in revised form 6 June 2006; accepted 13 December 2006
Available online 24 September 2007

Abstract

A typical approach to active control of sound radiation or transmission from vibrating structures involves active structural acoustic control (ASAC) and active noise control (ANC), which introduce respectively force input and compacted sound source to apply on or be close to the vibrating structure. However, for the ASAC approach, arrangement for secondary force and error sensor is heavily dependent upon the properties of the primary structure and acoustical space; for the ANC approach, a large number of compacted secondary sources are required. Hence, in this paper, based on distributed secondary sound source and near-field error sensor, active acoustic structure is proposed to construct adaptive or smart structure as a versatile module or element for controlling sound radiation or transmission at low frequencies. First, a theoretical model based on a minimization of the total sound radiation from the primary and secondary panel is established, after which, taking into consideration the relationship between the vibration modes pattern and sound radiation characteristics for secondary panels, optimal arrangement for the secondary panels is examined in detail. Finally, a near-field pressure-based error sensing approach is presented, based on two kinds of object function, and active control of sound radiation is performed.

1. Introduction

For actively controlling sound radiation or transmission from vibrating structures, a typical approach involves adding secondary force input applied directly on the radiating structure, termed as active structural acoustic control (ASAC) first proposed by Fuller [1]. However, the ASAC approach has many potential drawbacks, for example, reduction in the radiated sound power is closely related to secondary actuators/error sensors configuration, boundary conditions of radiating structures, and acoustical environments such as free field, enclosed field, etc. Therefore, there is no versatile secondary actuators/error sensors configuration such that it is impractical for the ASAC approach to be used to actively control the sound radiated from complex vibrating structures. Moreover, for heavy structures, direct force actuation requires large amounts of energy and may cause structural fatigue. Hence, the acoustic source control approach is especially attractive, which introduces secondary acoustic sources to suppress the unwanted noise, termed as active noise control (ANC).

*Corresponding author.

0022-460X/$ - see front matter © 2007 Published by Elsevier Ltd.
doi:10.1016/j.jsv.2006.12.027

In this case, simple sources such as loudspeakers, which can be modelled theoretically as monopole sources or dipole sources, are considered for use as the secondary sources [2]. It has been shown [2] that when the size of the vibrating structure producing the primary sound field is larger compared with an acoustic wavelength, a considerably large number of secondary sources is required to achieve sound reduction over a broad range of frequencies. Unfortunately, such an overly complicated secondary source configuration will impede practical applications.

More recently, based on the ANC approach, a new active control strategy using distributed acoustic actuators as secondary sources (termed secondary panels) was presented to construct an active acoustic structure (AAS) for reducing sound radiated from an original vibrating panel (termed primary panel) [3,4]. A theoretical model for AAS has been established [4] and, based on Madanik's "corner monopole" model [5], a preliminary investigation on physical mechanisms for active noise reduction has been given. However, detailed and qualitative analysis about the arrangement of the secondary structures and error sensing strategy was left unanswered.

The use of distributed secondary sound sources and near-field error sensors bonded and close to the primary panel is the key part of AAS. Although the active double panel (or skin) system that has been investigated by many researchers [6–9] has a similar configuration, its secondary actuators are limited to rectangular flexible panels [6–8] or a diaphragm [8], which is unrealistic for practical implementations. For AAS, the secondary structure represents distributed sound sources or typically planar loudspeakers, which have extensively been investigated [10–12] and have successful commercial applications in the field of audio-technology and further active control of sound [13,14]. Hence AAS may be developed to be a versatile element for attenuating low-frequency noise and independent of the primary vibrating structure and acoustic environments.

On the other hand, since AAS will be used as a noise control element independent of the primary structures, error sensors at a relatively far distance from the primary structure cannot be permitted such that the near-field error sensing is indispensable. In recent years, some near-field error sensing approaches in which piezoelectric patch, accelerator, PVDF film, etc. are used as sensing volume velocity, acceleration, and displacement have been developed to obtain vibration quantities related to radiated sound power [15–20]; however, for AAS a set of vibration sensors mounted or bonded on the primary panel or secondary panel cannot measure simultaneously sound radiation from the primary and secondary structure. Therefore, a near-field sound pressure-based sensing strategy is presented to constitute objective functions for adaptive active control. Additionally, it should be noted that in order to guarantee sound pressure reduction at far field for off-resonance cases, an error sensing strategy involved in direct use of squared pressures at a number of near-field locations [21] should be avoided and transformed near-field pressure will be used in this study.

In this paper, optimal configurations for the secondary panels and near-field error sensors are investigated theoretically. First, a theoretical model based on a minimization of the total sound radiation from the primary and secondary panel is given, after which, taking into consideration the relationship between the vibration modes pattern and sound radiation characteristics for secondary panels, optimal arrangement for the secondary panels is examined in detail. Finally, a near-field pressure-based error sensing approach is presented, based on two kinds of object functions, active control of sound radiation is performed, and then optimal arrangement for near-field sensors is examined from numerical examples.

2. Active control of sound radiated from planar structures

The primary sound field needed to be controlled is assumed to originate from a vibrating primary panel with simply supported boundary conditions and excited by an external force. L planar acoustic sources or secondary panels are introduced to produce the secondary sound field interfering destructively with the primary sound field. The secondary panels are parallel to the primary panel and softly mounted on the close proximity to the primary panel surface, and hence the vibrational energy flow between the primary and secondary panels can be ignored. For sound field analysis, all the secondary panels can be considered to locate on the same plane since the gap between the primary and secondary panels is much smaller than a wavelength of sound of interest.

The sound radiation from a vibrating panel can be assumed to be due to a number of elemental radiators, which are equivalent to small piston sources on a surface when the dimensions of the elements must be much

less in comparison to an acoustic wavelength. Let $\mathbf{V}$ denote the vector of normal velocity v_i ($i = 1,2,\ldots,N$); on the elemental radiator surface, the radiated power can be formulated as [16]

$$W = \mathbf{V}^H \mathbf{R} \mathbf{V}, \tag{1}$$

where $\mathbf{R} = \Delta S \mathrm{Re}(\mathbf{Z})/2$, and Re( ) is a real part of a complex variable, ΔS is the elemental area, and $\mathbf{Z}$ is an $N \times N$ acoustic transfer impedance matrix relating the complex pressure at every radiator to the complex velocity of every radiator, whose (i, j) element can be given by [22]

$$z(i,j) = \begin{cases} -\dfrac{j\rho_0 c_0 k \Delta S \mathrm{e}^{jkr_{ij}}}{2\pi r_{ij}}, & i \neq j, \\ \rho_0 c_0 \left(1 - \mathrm{e}^{jk\sqrt{\Delta S/\pi}}\right), & i = j, \end{cases} \tag{2}$$

where r_{ij} is the distance between the ith and jth element, ρ_0 and c_0 are the density and sound speed of the medium, and k is the wavenumber.

For the primary panel, defining the normal velocity vector as N-length vector $\mathbf{V}_p$, the radiated power can be given by $W_p = \mathbf{V}_p^H \mathbf{R} \mathbf{V}_p$. It is assumed that each of the secondary panels has the same size and is divided as M elemental radiators. Then, the normal velocity of the lth secondary panel is represented in vector form as $\mathbf{V}_{sl} = [v_{sl1}, v_{sl2}, \ldots, v_{slM}]^{\mathrm{T}}$ ($l = 1,2,\ldots,L$) and then a complex velocity vector related to L secondary panels can be denoted as $\mathbf{V}_s = [\mathbf{V}_{s1}^{\mathrm{T}} \quad \mathbf{V}_{s2}^{\mathrm{T}} \ldots \mathbf{V}_{sL}^{\mathrm{T}}]^{\mathrm{T}}$.

In order to calculate the total sound power radiated by both the primary and secondary panels, a new vector relating to the secondary panel is defined to match the dimensions of the velocity vector of the primary panel, i.e. $\mathbf{V}_{s0} = [\mathbf{V}_{s1}^{\mathrm{T}} \quad \mathbf{V}_{s2}^{\mathrm{T}} \ldots \mathbf{V}_{sL}^{\mathrm{T}} \quad \mathbf{O}^{\mathrm{T}}]^{\mathrm{T}} = [\mathbf{V}_s^{\mathrm{T}} \quad \mathbf{O}^{\mathrm{T}}]^{\mathrm{T}}$, where $\mathbf{O}$ is an M_2-length vector ($M_2 = N - M \times L$) with each component being equal to zero. When the secondary panels are actuated, the overall velocity from the primary and secondary panels can be superimposed linearly and expressed as $\mathbf{V} = \mathbf{V}_p + \mathbf{V}_{s0}$. Substituting this notation into Eq. (1) yields the total radiated power given by

$$W = W_p + W_s + W_{ps}, \tag{3}$$

where W_p is the sound power for the primary panel in the absence of the secondary panels, W_s is due to the secondary panels in the absence of the primary panel, and W_{ps} results from the interference of the sound field of the primary panel with that of the secondary panels. The expressions for W_s and W_{ps} can be expressed in terms of $\mathbf{V}_s$ as detailed in Ref. [4].

Based on the modal superposition approach, the normal velocity of a vibrating panel can be written as

$$v(\omega, x, y) = j\omega \sum_{n_x=1}^{N_x} \sum_{n_y=1}^{N_y} F_n A_n \phi_n(x, y), \tag{4}$$

where $n = (n_x, n_y)$ is a modal index along X and Y directions in the Cartesian coordinate system, $\phi_n(x, y)$ and A_n are a complex modal shape function at field point (x, y) and modal amplitude in association with geometric and material properties and boundary condition of the mechanical system, and F_n is called generalized modal force given by

$$F_n = \frac{1}{S} \iint_S \phi_n(x, y) f(x, y) \, \mathrm{d}x \, \mathrm{d}y, \tag{5}$$

where S is the area of the structural surface and $f(x, y)$ is an external applied force.

For the secondary panels, the external forces can be split into two parts: one is an input force from the output of an active controller; the other is a fluctuating sound pressure radiated from the primary panel. Thus, for the lth secondary panels, the applied forces can be expressed as follows:

$$f_{sl}(x, y) = f_{scl}(x, y) + f_{spl}(x, y), \tag{6}$$

where $f_{scl}(x, y)$ is the control force applied to the lth secondary panel and $f_{spl}(x, y)$ is from the primary panel.

Corresponding to Eq. (6), the normal velocity on the lth secondary panel can be written in vector form as

$$\mathbf{V}_{sl} = f_{l0}\mathbf{V}'_{scl} + \mathbf{V}_{spl} \quad (l = 1, 2, \ldots, L), \tag{7}$$

where f_{l0} is the complex strength for the control force applied to the lth secondary panel.

The use of Eqs. (4)–(6) derives respectively the component m of $\mathbf{V}'_{scl}$ and $\mathbf{V}_{spl}$ as follows:

$$v'_{scl,m}(x, y) = j\omega \sum_{n_x=1}^{N_x} \sum_{n_y=1}^{N_y} g_{n,scl} A_{n,s} \phi_{n,s}(x_{lm}, y_{lm}), \tag{8a}$$

$$v_{spl,m}(x, y) = j\omega \sum_{n_x=1}^{N_x} \sum_{n_y=1}^{N_y} F_{n,spl} A_{n,s} \phi_{n,s}(x_{lm}, y_{lm}), \tag{8b}$$

where

$$g_{n,scl} = \frac{1}{S_s} \phi_{n,s}(x_l, y_l) \tag{9}$$

and

$$F_{n,spl} = \frac{(\Delta S)^2 \rho_0 c_0^2}{j\omega l_{sp} S_s} \sum_{m=1}^{M} \phi_{n,s}(x_{lm}, y_{lm}) v_p(x_{lm}, y_{lm}), \tag{10}$$

where (x_{lm}, y_{lm}) are the central coordinates of the mth element on the lth secondary panel, l_{sp} is the distance of the gap between the primary and secondary panel, and S_s is the area of each secondary panel.

Since the normal velocity vector $\mathbf{V}_s$ relates directly with the complex strength of the secondary forces, all the control force acting on the secondary panel can be expressed in vector form as $\mathbf{F}_s = [f_{10}, f_{20}, \ldots, f_{L0}]^{\mathrm{T}}$, the corresponding normal velocity vector can be written as

$$\mathbf{V}_{sc} = \mathbf{F}_s \mathbf{V}'_{sc}, \tag{11}$$

and thus Eq. (7) can be rewritten as

$$\mathbf{V}_s = \mathbf{F}_s \mathbf{V}'_{sc} + \mathbf{V}_{sp}. \tag{12}$$

Substituting Eq. (11) into Eq. (1), we arrive at

$$W = \mathbf{F}_s^H \mathbf{A} \mathbf{F}_s + \mathbf{F}_s^H \mathbf{B} + \mathbf{B}^H \mathbf{F}_s + C, \tag{13}$$

where the matrix $\mathbf{A}$, $\mathbf{B}$, and constant C are related to $\mathbf{V}_p$, $\mathbf{V}_{sc}{}'$, and $\mathbf{V}_{sp}$ as detailed in Ref. [4]. It is shown from Eq. (13) that the total sound power is the quadratic form of the complex strength vector of the control force. Thus using the unconstrained optimization method [1,3], the solution to Eq. (13) can be given by $\mathbf{F}_{so} = -[\mathbf{B}^H \mathbf{B}]^{-1} \mathbf{B}^H \mathbf{A}$ and substituting this solution into Eq. (13) yields a minimum sound power output after active control as follows:

$$W_o = C - \mathbf{B}^H \mathbf{A}^{-1} \mathbf{B}. \tag{14}$$

3. Arrangements of secondary panels

3.1. Physical interpretations

It is known from G. Maidanik's 'corner monopole' model [14] that under coincidence frequency sound radiation from a vibrating panel can be approximated as that radiated from four point sources located on four corners. These point sources can be combined into monopole, dipole, and quadrapole sources corresponding to sound radiation from structural modes with (odd, odd), (odd, even) or (even, odd), and "even–even" indices.

In the AAS, each of the secondary panels behaves as a four 'corner monopole' situated at each corner; hence the radiation characteristics for one or multiple secondary panels can be considered to be equivalent to an array of monopole sources. Therefore, the mechanisms of active control of sound can also be interpreted using the monopole sources cancellation model. However, notice that the normal velocity of each of the secondary panels in AAS is constrained and directly controlled by one input force; thus, in this situation the effect of secondary panels arrangement on sound reduction will be greatly distinguished from simple secondary sources-based ANC approach, in which the strength of each monopole-like secondary source can be independently controlled [2].

In order to achieve substantial reduction in sound power, a minimum number of secondary monopole sources is required to match the radiation characteristics of the primary panel. For AAS, it is concluded [4] that (1) using one secondary panel, the sound power radiated by (odd, odd) structural modes can be reduced; (2) using two secondary panels, the sound power by not only (odd, odd) modes but also (odd, even) or (even, odd) modes can be reduced; and (3) using four secondary panels can guarantee considerable reduction in sound power radiated from any kind of structural mode.

Furthermore, in order to explore optimal configuration for secondary panels, the distribution pattern for structural modes should be taken into account. For planar radiators, it is well known that, for single structural mode, sound radiation is directly related to its velocity distribution and stronger radiated sound power results from larger normal velocity. Therefore, the secondary panel should be placed to coincide with an "antinodal surface" of the structural mode needed to be reduced. Here, the antinodal surface is a spatial region around the immediate vicinity of a crest or through the structural modal pattern. Moreover, the number of the secondary panels had better be the same as the number of the crest or through the structural mode.

3.2. Numerical examples

The primary panel is assumed to be a simple supported steel panel 6 mm in thickness; its length and width are $L_{xp} = 1.15$ m and $L_{yp} = 0.86$ m, respectively. A damping ratio for all structural modes is assumed to be 0.01, Young's modulus is 2.16×10^{11} N/m^2, density is 7.8×10^3 kg/m^3, and Poisson's ratio is 0.28. A point force is applied to the primary panel at $(-3L_{xp}/8, -3L_{yp}/8)$. The primary panels are equally spaced divided into 8 by 8 elemental radiators along the X and Y directions, 13 structural modes are included between 20 and 300 Hz, and the radiated power can be calculated by using Eq. (1) as shown in Fig. 1, in which the index of the structural modes has been labeled. The modal patterns for (1, 1), (2, 1), (2, 2), and (3, 3) modes are plotted and the antinodal surfaces can be observed in Fig. 2.

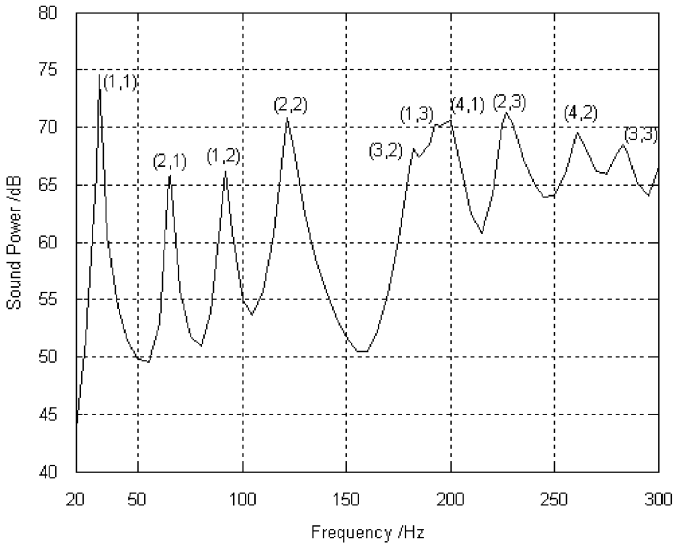

Fig. 1. Sound power radiated from the primary panel.

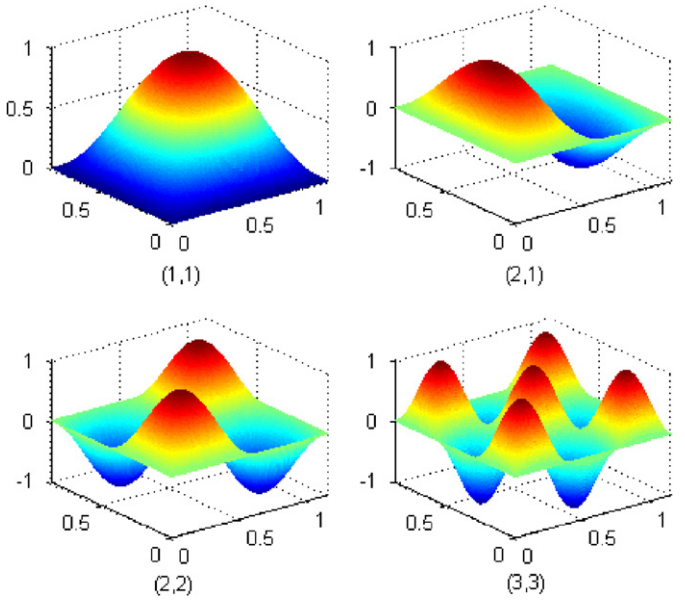

Fig. 2. Structural mode patterns for the primary panel.

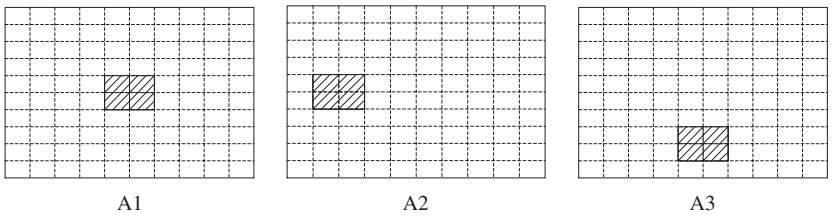

Fig. 3. Locations for the secondary panel.

All the secondary panels are considered as simply supported steel panels. Their dimensions are denoted respectively by L_{xs} and L_{ys}, and point forces acting on the secondary panels are placed at $(0.1L_{xs}, 0.1L_{ys})$. In simulations, the modal density for the secondary panels is chosen to be lower than that of the primary panel. In the following subsections, the arrangements for single and multiple secondary panels are considered.

3.2.1. Single secondary panel case

In this case, three kinds of secondary panel configurations, labeled respectively as A1, A2, and A3, are considered as shown in Fig. 3, in which the shadowed rectangular panels represent secondary panels and are divided into elemental radiators being the same size as that of the primary panel. Using the theoretical model given in Section 1, the sound power before and after active control using the single secondary panel with A1, A2, and A3 arrangement can be calculated as shown in Fig. 4. It is seen that only the sound power from (1, 1) structural mode can be effectively reduced and, in comparison with the modal pattern in Fig. 2, it is the secondary panel with A1 configuration being placed to coincide with the antinodal surface of (1, 1) mode that results in a substantial reduction in sound power of (1, 1) mode.

3.2.2. Multiple secondary panel case

For multiple secondary panels, more complicated configurations, labeled as B1–B4, are considered as shown in Fig. 5. It is noted that the secondary panel configurations with B1, B3, and B4 completely coincide with the antinodal surface corresponding respectively to (2, 1), (2, 2), and (3, 3) structural mode. Again using the theoretical model in Section 1, the sound power before and after control is calculated as shown in Fig. 6. It is proven again that if the secondary panel configurations are in agreement with the antinodal surfaces of

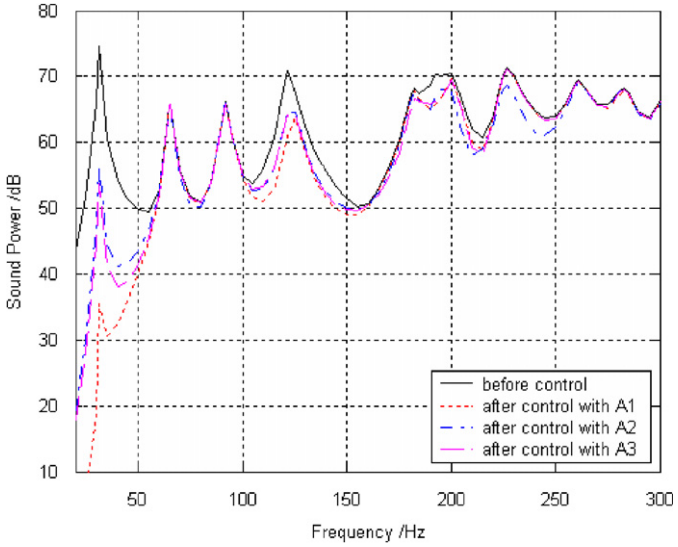

Fig. 4. Sound power before and after active control for different secondary panel arrangements.

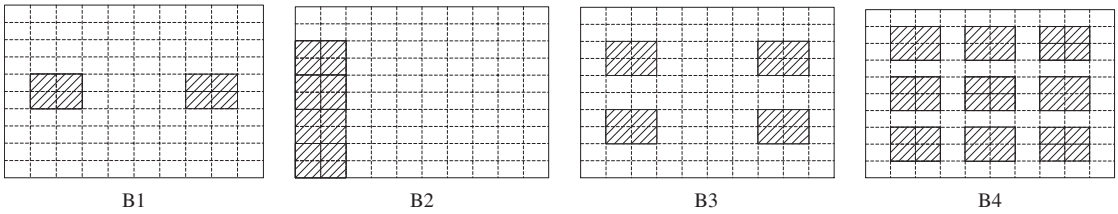

Fig. 5. Locations for multiple secondary panels.

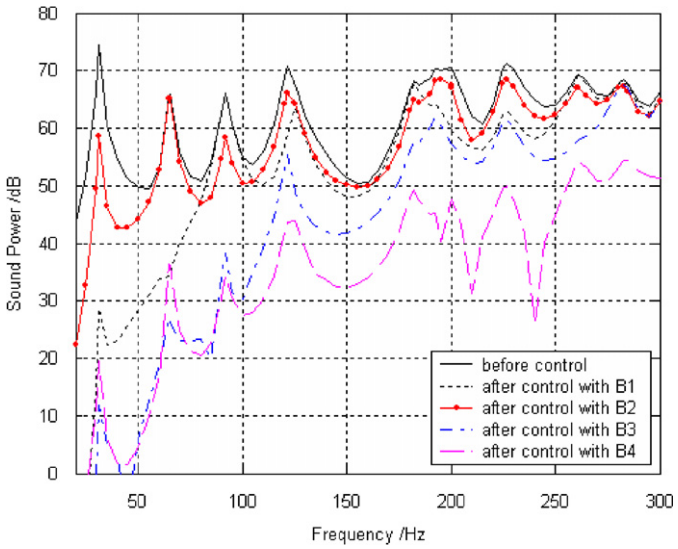

Fig. 6. Sound power before and after active control for different arrangements.

the structural modes, the corresponding sound power radiated from these structural modes can effectively be reduced. For example, the secondary panel configurations with B1 and B3 are consistent with the antinodal surface of the (2, 1) and (2, 2) mode such that a substantial reduction in sound power below the natural

frequency of the (2, 1) and (2, 2) modes can be achieved. Since the configuration B2 does not coincide with any antinodal surface, considerable reduction in sound power cannot be achieved over entire frequency below 300 Hz, whereas the configuration B4 corresponds to almost all the structural modes' antinodal surface in Fig. 2 such that the sound power below 300 Hz can be largely reduced.

4. Error sensing strategy based on near-field pressure sensing

Error sensors are indispensable to active control system and, as stated previously, near-field error sensing must be taken into consideration in the design of AAS. However, the most promising near field sensing strategies used in ASAC, involving measuring of strain [15], velocity [16,17], or acceleration of the structure, are not suitable to be applied to AAS, since the vibration transducers such as polyvinylidene fluoride films (PVDF) [20] do not measure simultaneously quantities related to the radiated sound power from the primary panel and secondary panels. However, the microphone located very close to the surface of the secondary panels can measure the sound pressure radiated from not only the primary panel but also the secondary panels. Accordingly, in the following sections, near-field pressure measurement is used to estimate the radiated sound power and construct an objective function to be minimized.

4.1. Radiated sound power estimation based on near-field sound pressure

Assume that a vibrating panel is divided into N elemental radiators as described in Section 1 and let $\mathbf{P}$ denote the pressure vector with components p_i ($i = 1,2,\ldots,N$) being close to the surface of the elemental radiator. Then the relationship between pressure and normal velocity can be formulated in the form of vector as

$$\mathbf{P} = \mathbf{Z}\mathbf{V} \tag{15a}$$

or

$$\mathbf{V} = \mathbf{Y}\mathbf{P}, \tag{15b}$$

where $\mathbf{Y}$ is an inverse of $\mathbf{Z}$ termed a mobility matrix. Substituting Eq. (14b) into Eq. (1) leads to

$$W = \mathbf{P}^H\mathbf{G}\mathbf{P}, \tag{16}$$

where

$$\mathbf{G} = \Delta S\mathrm{Re}(\mathbf{Y})/2. \tag{17}$$

It follows from Eq. (16) that the radiated sound power can be expressed in terms of a discrete number of sound pressures close to the vibrating structure, called near-field pressures. From the point of view of active control, the direct use of Eq. (16) as an objective function will involve a considerable amount of computation in the active control algorithms due to matrix inverse in Eq. (15b), such that it is necessary to modify the expression of Eq. (16).

It is readily understood from Eq. (16) that the matrix $\mathbf{G}$ must be positive definite on physical grounds since the radiated sound power W is always greater than zero unless the pressure vector is zero. Because the matrix $\mathbf{Z}$ is symmetric, the matrix $\mathbf{G}$ must be purely real and also symmetric and positive definite such that the following eigen-decomposition can be conducted:

$$\mathbf{G} = \mathbf{D}^{\mathrm{T}}\Lambda\mathbf{D}, \tag{18}$$

where $\mathbf{D}$ is an $N \times N$ real and orthogonal matrix whose nth column, $\mathbf{d}_n$, is the nth real eigenvector and Λ is a diagonal matrix with positive real numbers eigenvalue λ_n. Substituting Eq. (18) into Eq. (16) and defining

$$\mathbf{P}_d = \mathbf{D}^{\mathrm{T}}\mathbf{P}, \tag{19}$$

we arrive at

$$W = \mathbf{P}_d^H\Lambda\mathbf{P}_d = \sum_{n=1}^{N}\lambda_n|p_{dn}|^2, \tag{20}$$

where $p_{dn} = \mathbf{d}_n^{\mathrm{T}}\mathbf{P}$ is a transformation of the pressure vector weighted by an eigenvector. Eq. (19) illustrates that the radiated power can be expressed as a summation of independent acoustic modes, termed in this paper as pressure radiation mode (or radiation mode in abbreviation), and the two-dimensional surface plotted with $\mathbf{d}_n$ is also called radiation mode shape. Using this notation, it is deduced that the total radiation comes from the power of the pressure radiation mode, each of which is independent. From the point of view of noise control, if any of the radiation modes is reduced, the total radiated sound power will be reduced correspondingly. In addition, in order to describe sound radiation capacity, the radiation efficiency for the nth radiation mode is defined as

$$\sigma_n = \frac{\lambda_n}{\mathrm{tr}[\mathbf{G}]}, \tag{21}$$

where tr[ ] is a trace of the matrix.

4.2. Active control of radiated sound based on near-field pressures sensing

In the following subsections, two kinds of objective function are proposed for use as active control strategies.

4.2.1. Minimization of the radiated sound power

As stated previously, the normal velocity produced by the secondary panel relates directly with the secondary forces, and the relation between $\mathbf{V}_s$ and $\mathbf{F}_s$ can be rewritten as

$$\mathbf{V}_s = \mathbf{T}\mathbf{F}_s, \tag{22}$$

in which $\mathbf{T} = \{t(i, j)\}_{N\times J}$ is a coefficient matrix. While the secondary forces are applied, the resulting velocity vector originating from both the primary and secondary panel can be written as

$$\mathbf{V} = \mathbf{V}_p + \mathbf{V}_s, \tag{23}$$

where $\mathbf{V}_p$ is the velocity vector of the primary panel. In correspondence with Eq. (23), the total near-field sound pressure vector can be given by

$$\mathbf{P} = \mathbf{P}_p + \mathbf{P}_s. \tag{24}$$

It is shown from Eq. (23) that when the secondary force is applied, in order to obtain the total velocity, two sets of velocity sensors are required to respectively measure $\mathbf{V}_p$ and $\mathbf{V}_s$. However, under some practical situations it is difficult to measure the primary velocity $\mathbf{V}_p$. According to Eq. (24) only one set of acoustic sensors close to the secondary structure can measure simultaneously $\mathbf{P}_p$ and $\mathbf{P}_s$. This is one of the reasons why the near-field pressures are used as the error signal in AAS.

While the near-field pressure is measured, the objective function for active control can be constructed as follows:

$$J_p = \mathbf{P}^H\mathbf{G}\mathbf{P}. \tag{25}$$

After substituting Eq. (15), Eqs. (22)–(24) into Eq. (25), it is found that J_p is a quadrature function of the complex strength vector $\mathbf{F}_s$. Therefore, using the unconstrained optimization method the optimal secondary force strength and corresponding radiated sound power can be yielded as follows:

$$\mathbf{F}_{spo} = -\mathbf{A}_p^{-1}\mathbf{B}_p, \tag{26}$$

$$W_{po} = C_p + \mathbf{B}_p^H\mathbf{F}_{spo}, \tag{27}$$

where $\mathbf{A}_p = \mathbf{T}^H\mathbf{Z}^H\mathbf{G}\mathbf{Z}\mathbf{T}$, $\mathbf{B}_p = \mathbf{T}^H\mathbf{Z}^H\mathbf{G}\mathbf{P}_p$, and $C_p = \mathbf{P}_p^H\mathbf{G}\mathbf{P}_p$.

4.2.2. Minimization of the sound power for dominant radiation modes

In practice, if J_p in Eq. (25) is used as the objective function, the corresponding adaptive active control algorithm will become considerably complicated. Thus the radiated sound power in terms of Eq. (25) can only be viewed as a theoretical and ideal objective function.

As indicated in Eq. (20), the total radiated sound power can be approximated as linear summation from a finite number of independent modal power. It has been shown from numerical examples that at most the first six radiation modes are dominant in the low-frequency range, and at the extreme the first mode is the only efficient mode. This motivates the use of the sound power for the low-order radiation modes to act as the objective function for active control. It is anticipated that, for the nth radiation mode whose power is chosen as the objective function, the larger the radiation efficiency σ_n, the better the effectiveness of the reduction in sound power.

Assume that there are K dominant radiation modes. Corresponding radiation pressures can be denoted as $\mathbf{P}_k = \mathbf{D}_k\mathbf{P}$, where $\mathbf{D}_k = [\mathbf{d}_1,\mathbf{d}_2,\ldots,\mathbf{d}_K]^{\mathrm{T}}$. Since the sound power due to the dominant modes can be viewed as the approximation of the total sound power given by Eq. (1), the objective function can be expressed as

$$J_k = \mathbf{P}_k^H \Lambda_k \mathbf{P}_k = \sum_{n=1}^{K} \lambda_{kn} |p_{kn}|^2, \tag{28}$$

where $\Lambda_k = \mathrm{diag}(\lambda_1, \lambda_2, \ldots, \lambda_K)$.

Again using the unconstrained optimization method, the optimal secondary force strength can be deduced as follows:

$$\mathbf{F}_{sko} = -\mathbf{A}_k^{-1}\mathbf{B}_k, \tag{29}$$

where $\mathbf{A}_k = \mathbf{T}^H\mathbf{Z}^H\mathbf{D}_k^H\Lambda_k\mathbf{D}_k\mathbf{Z}\mathbf{T}$, $\mathbf{B}_k = \mathbf{T}^H\mathbf{Z}^H\mathbf{D}_k^H\Lambda_k\mathbf{P}_{pk}$, and $\mathbf{P}_{pk} = \mathbf{D}\mathbf{P}_p$.

Substituting for $\mathbf{F}_{sko}$ into Eq. (20) yields the minimum radiated sound power after active control and we have

$$W_{ko} = \mathbf{P}_{k0}^H \Lambda \mathbf{P}_{k0}, \tag{30}$$

where

$$\mathbf{P}_{ko} = \mathbf{P}_p + \mathbf{Z}\mathbf{T}\mathbf{F}_{sko}. \tag{31}$$

4.2.3. Numerical examples

If the secondary panels are excited by point forces located respectively at (x_{sj}, y_{sj}) $(j = 1,2,\ldots,J)$, the (i, j) component of the coefficient matrix $\mathbf{T}$ can be derived as follows:

$$t(i,j) = \frac{j\omega}{S}\sum_{m=1}^{M} A_m(\omega)\phi_m(x_i,y_i)\phi_m(x_{sj},y_{sj}), \tag{32}$$

where (x_i, y_i) is the position of the elemental radiators i.

In this simulation, one secondary panel is considered. The physical and geometrical parameters are chosen to be the same as that in Section 3.2. It is shown from the calculation of the radiation efficiency that at low frequencies below 100 Hz, the radiated power for the first radiation mode is predominant and when the excited frequency is gradually increased the other low-order radiation modes' contribution to the radiated sound power is also increased. Actually, only the first four modes are dominant pressure radiation modes below 300 Hz.

Next, active control-based near-field pressure sensing is examined. Firstly, consider that the total radiated sound power J_p in Eq. (25) and the sound power for finite dominant radiation modes J_k in Eq. (28) are respectively used as the objective function. Then after control the residual sound power can be calculated as shown in Fig. 7, in which the radiated sound power before and after control are denoted respectively by real line, dotted line, and dashed line. In dashed line the sound power for the first two dominant modes is used as the objective function and it is shown that in this case the sound power reduction is approximately equal to that in the case of J_p unless at some natural frequencies. In fact, more simulation results show that, using respectively the total radiated power and the radiated power for the first four radiation modes, i.e. J_p and J_k, as objective functions, reductions in the radiated sound power are basically the same.

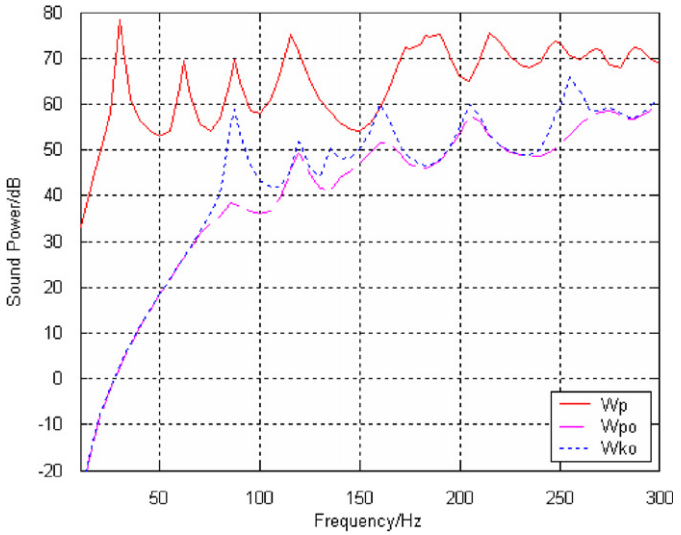

Fig. 7. Sound power before and after active control with J_p and J_k minimization.

5. Conclusions

AAS with distributed secondary sources and near-field error sensors is proposed to actively control low-frequency sound radiation from vibrating structures. In this paper, optimum arrangements for secondary panels and near-field error sensing strategies are investigated theoretically. In principle, at least four secondary panels are required to effectively control any kind of sound radiation from the vibrating structure. Further, for active control of sound from a certain structural mode the secondary panels must be placed to coincide with the antinodal surface for such a structural mode. With respect to the error sensing, sound pressures in the near-field of the primary and secondary panels are used to construct the objective function for active control. Because the total sound power is decomposed into a finite number independent power relating with the radiation modes and only a few of which is dominant, dominant radiation modes can be used to obtain error signal in the active control process. It has been shown that, in the low-frequency range, if the dominant radiation modes (at most the first four radiation modes) are controlled, substantial reduction in the total sound power can be achieved. Additionally, if J_k is chosen as the objective function, each component of near-field pressure-based radiation modes can be used as the error signals in the multichannel active control algorithms such as multichannel filtered-X LMS (FxLMS). For practical applications, fast implementation of multichannel algorithms must be taken into account. Meanwhile, causality and stability problems in the design of the active controller must be carefully considered.

Acknowledgements

The first author gratefully acknowledges the support of this work by the National Natural Science Foundation of China under Grant no. 10274060, the Aeronautic Science Foundation of China under Grant no. 01I50307, and International Cooperation Program for Akita Prefectural University, Akita, Japan.

References

[1] C.R. Fuller, S.J. Elliott, P.A. Nelson, *Active Control of Vibration*, Academic Press, San Diego, 1996.
[2] C. Deffayet, P.A. Nelson, Active control of low-frequency harmonic sound radiated by a finite panel, *Journal of Acoustic Society of America* 84 (1988) 2192–2199.
[3] K. Chen, *Active Noise Control*, National Defense Industry Press, Beijing, 2003 (in Chinese).

[4] K. Chen, G.H. Koopmann, Active control of low-frequency sound radiation from vibrating panel using planar sound sources, *Journal of Vibration and Acoustics* 124 (2002) 2–9.
[5] G. Maidanik, Response of ribbed panels to reverberant acoustic fields, *Journal of the Acoustical Society of America* 34 (1962) 809–826.
[6] X. Pan, T.J. Sutton, S.J. Elliott, Active control of sound transmission through a double-leaf partition by volume velocity cancellation, *Journal of the Acoustical Society of America* 104 (1998) 2828–2835.
[7] J.P. Carneal, C.R. Fuller, An analytical and experimental investigation of active structural acoustic control of noise transmission through double panel systems, *Journal of Sound and Vibration* 272 (2004) 749–771.
[8] J. Pan, C. Bao, Analytical study of different approaches for active control of sound transmission through double walls, *Journal of the Acoustical Society of America* 103 (1998) 1916–1922.
[9] B.D. Johnson, C.R. Fuller, Broadband control of plate radiation using a piezoelectric, double-amplifier active-skin and structural acoustic sensing, *Journal of the Acoustical Society of America* 107 (2000) 876–884.
[10] E.Y. Prokofieva, K. Horoshenkov, The acoustic emission of a distributed mode loudspeaker near a porous layer, *Journal of the Acoustical Society of America* 111 (2002) 2665–2670.
[11] R. Heydt, R. Pelrine, J. Joseph, J. Eckerle, R. Kornbluh, Acoustical performance of an electrostrictive polymer film, *Journal of the Acoustical Society of America* 107 (2000) 833–839.
[12] M. Paajanen, H. Valimaki, J. Lekkala, Modelling the electromechanical film (EMFi), *Journal of Electrostatics* 48 (2000) 193–204.
[13] H. Nykanen, M. Antila, J. Kataja, J. Lekkala, S. Uosukainen, Active control of sound based on utilizing EMFi technology, *Proceedings of ACTIVE'99*, FL, USA, 1999, pp. 22–36.
[14] H. Zhu, R. Rajamani, K.A. Steison, Active control of acoustic reflection, absorption and transmission using thin panel speakers, *Journal of the Acoustical Society of America* 113 (2003) 852–870.
[15] A.P. Berkhoff, Sensor scheme design for active structural acoustic control, *Journal of the Acoustical Society of America* 108 (1994) 1037–1045.
[16] M.E. Johnson, S.J. Elliott, Active control of sound radiation using volume velocity cancellation, *Journal of the Acoustical Society of America* 98 (1995) 2174–2186.
[17] T.C. Sors, S.J. Elliott, Volume velocity estimation with accelerometer arrays for active structural acoustic control, *Journal of Sound and Vibration* 258 (2002) 867–883.
[18] J.P. Maillard, C.R. Fuller, Advanced time-domain wave-number sensing for structural acoustic systems, I: theory and design, *Journal of the Acoustical Society of America* 95 (1994) 3252–3261.
[19] P. Masson, A. Berry, J. Nicolas, Active structural acoustic control using strain sensing, *Journal of the Acoustical Society of America* 102 (1997) 1588–1599.
[20] F. Charette, A. Berry, C. Guigou, Active control of sound radiation from a plate using a polyvinylidene fluoride volume displacement sensor, *Journal of the Acoustical Society of America* 103 (1998) 1493–1503.
[21] A. Berry, X. Qiu, C.H. Hansen, Near-field sensing strategies for the active control of the sound radiated from a plate, *Journal of the Acoustical Society of America* 106 (1999) 3394–3406.
[22] M.R. Bai, M. Tsao, Estimation of sound power of baffled planar sources using radiation matrices, *Journal of the Acoustical Society of America* 112 (2002) 876–883.